Available online at www.ijpe-online.com

International Journal of Performability Engineering

vol. 14, no. 3, March 2018, pp. 413-424
DOI: 10.23940/ijpe.18.03.p2.413424

Bearing Fault Diagnosis based on Stochastic Resonance with Cuckoo Search

Kuo Chi*, Jianshe Kang, Xinghui Zhang, and Zhiyuan Yang

Mechanical Engineering College, Shijiazhuang, 050003, China

Abstract

Rolling bearings are the main components of modern machinery, and harsh operating environments often make them prone to failure. Therefore, detecting the incipient fault as soon as possible is useful for bearing prognostics and health management. However, the useful feature information relevant to the bearing fault contained in the vibration signals is weak under the influence of the noise and transmission path. The useful feature information is even submerged in the noise. Thus, it becomes difficult to identify the fault symptom of rolling bearings in time from the vibration signals. Stochastic resonance (SR) is a reliable method to detect the weak signal in intense noise. However, the effect of SR depends on the adjustment of two parameters. Cuckoo Search (CS) is a heuristic novel optimization algorithm that can search the global solution quickly and efficiently. Thus, CS is utilized to optimize the two parameters in this paper. Local signal-to-noise ratio (LSNR) is used to evaluate resonance effect. Two bearing fault datasets were used to confirm the effectiveness of SR optimized by CS. SR methods optimized by particle swarm optimization (PSO), genetic algorithms (GA), firefly algorithm (FA), and ant colony optimization (ACO) are also used to detect the bearing fault signal in the two datasets. The analysis results state SR optimized by CS can find better LSNR than SR optimized by other algorithms no matter if it is in the same iterations or in the same computation time, thereby making the fault feature more obvious.

Keywords: rolling bearing; fault diagnosis; stochastic resonance; cuckoo search

(Submitted on October 12, 2017; Revised on December 8, 2017; Accepted on December 29, 2017)

1. Introduction

Bearings are an essential part of mechanical transmission systems (such as gearboxes), which are mainly used to support rotating parts of machines. A leading cause of mechanical transmission system failure is bearing failure. Bearing failure will affect the system transmission accuracy. Severe bearing failure even causes a catastrophic incident. If bearing failure is found earlier, maintenance personnel will have more preparation time to avoid the occurrence of the accident. Therefore, it is crucial to detect and diagnose bearing failures as early as possible.

Noise is intense and vibration transmission path is long. These conditions make the useful information about bearing fault weak. So, the bearing fault symptom is hard to diagnose promptly. Enhancing the bearing signal is necessary. These methods of enhancing the bearing signal include minimum entropy deconvolution (MED) [9], kurtosis method (like spectral kurtosis (SK), kurtogram) [36,37], and empirical mode decomposition (EMD) [38]. Randall [26] introduces these methods systematically. Current research tends to improve a method or a mixture of different methods. Sawalhi [27] combines MED with SK to enhance the rolling bearing failure. Raj [25] combines EMD with wavelet de-noising for fault diagnosis of bearings. Although much work has been done, there are still many shortcomings in bearing fault diagnosis. The useful information about bearing fault is too weak and submerged in a large number of noise backgrounds, especially at the beginning of bearing deterioration. Therefore, bearing incipient fault diagnosis is still a problem.

Stochastic resonance (SR) was first proposed by Benzi et al. [3] in 1981. SR is a signal enhancement phenomenon through the synergistic effect of the nonlinear system, noise, and signal. If the nonlinear system and noise are proper, the noise will transfer some energy to the signal through the nonlinear system, and the signal will be enhanced and have a better signal-to-

* Corresponding author.
E-mail address: chimingshu@foxmail.com

noise ratio (SNR). Since SR was put forward, it has been studied and applied in many fields. In the field of bioengineering, Bates et al. [2] found SR in an intracellular genetic perceptron. In the field of image engineering, Yang et al. [34] investigate two-dimensional parameter-induced SR and apply it to filter out the Gaussian noise in the image. In the field of signal transmission, Duan [6] found the parameter-induced SR phenomenon in the baseband binary pulse amplitude modulated signals transmission. In the field of mechanical fault diagnosis, Hu et al. [11] studied the detection method of weak characteristic signals based on SR and applied it in the early diagnosis of mechanical faults.

According to adiabatic approximation theory [21], traditional SR can only deal with small-parameter signals (signal angular frequency $\omega_0 \ll$ Kramers Rate (KR), signal amplitude $A \ll 1$, noise intensity $D \ll 1$). In the mechanical fault diagnosis, the fault signals are usually large-parameter signals. So, traditional SR is unusable in mechanical fault diagnosis. To overcome this problem, some large-parameter SR methods are proposed, such as SR based on frequency information exchange [17], re-scaling frequency SR (RFSR) [14] (also called two sampling SR), parameters normalized SR [35], modulated SR [16], frequency-shifted and re-scaling SR [29]. SR based on frequency information exchange swaps the information in the small-parameter frequency domain with the information of the high-frequency target signal, and the target signal can be enhanced and detected by SR in the small-parameter frequency domain. Other methods transform large-parameter signals into small-parameter signals to satisfy adiabatic approximation limitation. Parameters normalized SR is simple and will be introduced in this paper.

The effect of SR depends not only on the noise intensity, but also on the parameters of the nonlinear system. Taking bi-stable system as an example, the two parameters of the system determine the height of the barrier. When the barrier is too high, the particle is difficult to transfer from one potential well to the other, and the bi-stable stochastic resonance is difficult to trigger. When the barrier is too low, the effect of SR is not apparent. Therefore, it is critical to choose the appropriate barrier height. Intelligent optimization algorithms, such as genetic algorithm (GA) [8], particle swarm optimization (PSO) [24], firefly algorithm (FA) [19], and ant colony optimization (ACO) [5] can search for excellent solutions through heuristic methods and have begun to apply in SR. Lei et al. [13] use a quantum GA to optimize the parameters of the multi-stable system and apply it to the fault diagnosis of rolling bearings. Zhang et al. [39] use PSO to optimize the step size of SR. Lei et al. [12] use ACO to optimize the parameters of the bi-stable system and apply it to the fault diagnosis of planetary gearboxes. However, these algorithms have relatively long computing times and are easily fall into a local optimum.

Cuckoo search (CS) was proposed by Yang and Deb [32] in 2009. Due to its excellent global optimization ability, CS and its improved algorithms have brought real application effects in many types of research, such as parameter estimation [4], face recognition [22] and image de-noising [20]. For instance, Chi [4] used CS to estimate the parameters of Weibull mixtures for reliability assessment. Naik [22] used adaptive CS for face recognition. Ouaarab [23] solved the traveling salesman problem by using discrete CS. In this paper, a novel adaptive SR based on CS is proposed and applied to bearing fault diagnosis. In section 2, the classical bi-stable SR is introduced. Then, parameters normalized SR will be analyzed to realize SR for large-parameter signals. An objective function has to be built for evaluating the SR effect. Section 3 introduces CS with Lévy flights, and pseudo code of CS for optimizing the parameters of SR is analyzed. Section 4 testifies the performance of our proposed method with two datasets of bearing faults and presents the computational results. Finally, Section 5 provides the conclusions.

2. Bi-stable SR Theory

2.1. Bi-stable SR

The fundamental of the bi-stable SR phenomenon is as follows: periodic signal and random noise drive a particle in a proper bi-stable system, and the proper noise assists in the enhancement of the oscillation. Langevin Equation (LE) is often used to describe this phenomenon as shown in Equation (1).

$$\frac{\mathrm{d}x}{\mathrm{d}t} = -V'(x) + S_{\mathrm{d}}(t) + N(t) \tag{1}$$

where, $S_{\mathrm{d}}(t)=A\cdot s(2\pi f_{\mathrm{d}}t+\varphi)$ is the periodic driving signal, $s(2\pi f_{\mathrm{d}}t)$ is a periodic signal with the frequency f_{d} and amplitude=1, A is the amplitude gain. $N(t)=\sqrt{2D}\cdot\varepsilon(t)$ is the Gaussian white noise (GWN) with noise intensity D. $\varepsilon(t)$ is a standard GWN (Mean value=0, and variance=1). $V(x)$ is the potential function of bi-stable SR:

$$V(x) = -\frac{a}{2}x^2 + \frac{b}{4}x^4 \tag{2}$$

where, $a>0$ and $b>0$ are the barrier parameters. When $x=\pm\sqrt{a/b}$, the potential function $V(x)$ achieves the min value $-\Delta V$, $\Delta V=a^2/4b$. Then the Equation (1) can be rewritten as:

$$\frac{\mathrm{d}x}{\mathrm{d}t}=ax-bx^3+A\bullet s\left(2\pi f_{\mathrm{d}}t+\varphi\right)+\sqrt{2D}\bullet\varepsilon\left(t\right) \tag{3}$$

When $s(2\pi f_{\mathrm{d}}t+\varphi)=\sin(2\pi f_0 t)$, Gammaitoni et al. [7] give the response of Equation (3):

$$\begin{cases}\left\langle x\left(t\right)\right\rangle=\overline{x}\sin\left(2\pi f_0-\overline{\phi}\right)\\ \overline{x}=\dfrac{A}{D}\dfrac{a}{b}\dfrac{r_K}{\sqrt{r_K^2+\pi^2 f_0}},\quad r_K=\dfrac{a}{\sqrt{2}\pi}\exp\left(-\dfrac{a^2}{4bD}\right)\\ \overline{\phi}=\arctan\left(\dfrac{\pi f_0}{r_K}\right)\end{cases} \tag{4}$$

where $\left\langle x\left(t\right)\right\rangle$ is the response of the system to the periodic driving signal; $\overline{x}$ is the amplitude; $\overline{\phi}$ is the phase lag; r_{K} is the Kramers rate.

2.2. Parameters Normalized SR

According to adiabatic approximation theory, SR will not realize unless the periodic signal satisfies the small-parameter limitation, which requires that signal amplitude $A\ll 1$, driving frequency $f_{\mathrm{d}}\ll r_K/2\pi^2$ and noise intensity $D\ll 1$. In engineering practice, the actual signals almost do not satisfy the requirement of SR. Thus, some strategies called large-parameter SR (LPSR) are used to process these large-parameter signals to satisfy the small-parameter limitation. In this article, a kind of LPSR called normalized scale transformation is used to process the large-parameter signals. Supposing that $z=\sqrt{a/b}\cdot x$ and $\tau=at$, Equation (3) becomes:

$$\frac{\mathrm{d}z}{\mathrm{d}\tau}=z-z^3+\sqrt{\frac{b}{a^3}}\left[As\left(\frac{2\pi f}{a}\tau\right)+N\left(\frac{\tau}{a}\right)\right] \tag{5}$$

Equation (5) is the normalized scale transformation of Equation (3), and they both are equal. After normalized scale transformation, the periodic signal frequency is reduced by a times, and the amplitude reduces $\sqrt{b/a^3}$ times. Therefore, the large-parameter signal would be changed into a small-parameter signal by normalized scale transformation with the appropriate parameter a and b, which can satisfy small-parameter limitation of SR.

In the engineering background, the vibration signal is an acceleration signal, which is the mixture of fault characteristic signal and noise. Let S indicate the acceleration signal, which is the mixture of the periodic signal $S_{\mathrm{d}}(t)$ and the noise $N(t)$: $S=S_{\mathrm{d}}(t)+N(t)$. Five order Runge-Kutta algorithm is adopted to solve Equation (5), as Equation (6).

$$\begin{cases}z_{n+1}=z_n+\dfrac{H}{6}\left[k_1+k_2+2k_3+k_4+k_5\right]\\ k_1=z_n-{z_n}^3+K\times S\left(n\right)\\ k_2=\left(z_n+\dfrac{H}{2}k_1\right)+\left(z_n+\dfrac{H}{2}k_1\right)^3+K\times S\left(n\right)\\ k_3=\left(z_n+\dfrac{H}{2}k_2\right)+\left(z_n+\dfrac{H}{2}k_2\right)^3+K\times S\left(n+1\right)\\ k_4=\left(z_n+\dfrac{H}{2}k_3\right)+\left(z_n+\dfrac{H}{2}k_3\right)^3+K\times S\left(n+1\right)\\ k_5=\left(z_n+Hk_4\right)+\left(z_n+Hk_4\right)^3+K\times S\left(n+1\right)\end{cases} \tag{6}$$

where $K=\sqrt{b/a^3}$ is the conversion factor of signal amplitude; $H=a/f_s$ is the time resolution after signal transformation, which is also considered as the integral time-step; z_n is the system output. Parameters H and K in Equation (6) determine the system output z_n. If H and K are changed, z_n will change too. In this paper, numerical solutions will be solved by Equation (6).

2.3. Objective Function

Index must be used to evaluate whether the SR has been triggered. A set of indexes include local signal-to-noise ratio (LSNR), SNR, SNR gain, weighted kurtosis index, and weighted power spectrum kurtosis (WPSK) [15,18,30]. SNR, LSNR, and SNR gain are the most commonly used indexes because they have precise definitions and are applied readily [10,12,28]. LSNR will be used as the index in this paper and it is defined as the ratio of the power of the meaningful signal and the power of background noise at the same frequency of the meaningful signal. For the discrete signal $x(k)$, LSNR can be calculated by Equation (7).

$$\begin{cases} LSNR = 10\log\dfrac{S(f_0)}{N(f_0)} \\ S(f_0) = \left|X(k_0)\right|^2 \\ N(f_0) = \dfrac{1}{2M}\sum\limits_{j=1}^{M}\left(\left|X(k_0-j)\right|^2 + \left|X(k_0+j)\right|^2\right) \end{cases} \tag{7}$$

Where $S(f_0)$ is the power of frequency f_0; $N(f_0)$ is the mean power of frequencies near f_0; f_0 is the concerned frequency (f_0 is frequency of periodic driving signal f_d for SR or the failure frequency for bearings); $X(k)$ is the Fast Fourier Transform (FFT) of discrete signal $x(k)$; k_0 is the number of frequency f_0, which means that $f_0/f_s=k_0/(N\text{-}1)$, f_s is the sampling frequency; M is appropriately selected according to signal length and sampling frequency.

Because of the leakage of signal and the difficulty of finding a spectrum line whose frequency is just equal to f_0, Equation (7) is adequately modified as Equation (8).

$$\begin{cases} LSNR = 10\log\dfrac{S_R(f_0,\Delta f_0)}{N_R(f_0,\Delta f_N)} \\ S_R(f_0,\Delta f_0) = \sum\limits_{j=k_1}^{k_2}\left|X(j)\right|^2 \\ N_R(f_0,\Delta f_N) = \sum\limits_{j=k_3}^{k_4}\left|X(j)\right|^2 - \sum\limits_{j=k_1}^{k_2}\left|X(j)\right|^2 \\ k_j = i, \text{if } \min\limits_{i=0}^{N-1}\left|\dfrac{if_s}{N-1} - f_j\right|, j = 1,2,3,4 \\ f_1 = f_0 - \Delta f_0,\ f_2 = f_0 + \Delta f_0, \\ f_3 = f_0 - \Delta f_N,\ f_4 = f_0 + \Delta f_N, \text{if } f_0 \ge \Delta f_N \\ f_3 = 0,\ f_4 = 100, \text{if } f_0 \ge \Delta f_N \\ 0 < \Delta f_0 < \Delta f_N \end{cases} \tag{8}$$

where $S_R(f_0, \Delta f_0)$ is the power in frequency domain $[f_0\text{-}\Delta f_0, f_0\text{+}\Delta f_0]$; $N_R(f_0, \Delta f_N)$ is the power in frequency domain $[f_0\text{-}\Delta f_N, f_0\text{-}\Delta f_0)\cup(f_0\text{+}\Delta f_0, f_0\text{+}\Delta f_N]$; Δf_0 and Δf_N can be chose properly according to signal length and sampling frequency f_s, $\Delta f_0<\Delta f_N$. In this paper, we set the parameters as follows: Δf_0=0.5 Hz and Δf_N=50 Hz, if $f_0\ge$50 Hz; Δf_0=0.5 Hz and $[f_0\text{-}\Delta f_N, f_0\text{-}\Delta f_0)\cup(f_0\text{+}\Delta f_0, f_0\text{+}\Delta f_N]=[0, f_0\text{-}\Delta f_0)\cup(f_0\text{+}\Delta f_0, 100]$, if $f_0<$50 Hz.

In practice, it can be said that the processed signal is better than the input signal only when LSNR of the processed signal is larger than the input signal. If LSNR of the processed signal is the largest, the processed signal is regarded as the best. According to this idea, the objective function is built as:

$$\max LSNR\left[z(H,K)\right] \tag{9}$$

where z(H, K) is the system output by Equation (6); H and K are the same as Equation (6).

3. Cuckoo Search by Lévy Flights

Proper nonlinear system and proper noise can both assist in the enhancement of the signal. Due to the excellent global optimization ability, CS and its improved algorithms have brought real application effects in various research. In this paper, CS by Lévy flights is applied to seek the optimal parameters of the bi-stable system to realize SR. Lévy flight is an efficient strategy for path search and will be introduced in subsection 3.1. Then, CS will be analyzed in subsection 3.2. Subsection 3.3 will introduce the primary technical process of our proposed method for bearing fault diagnosis.

3.1. Lévy Flights

Lévy flights have been found in many cases, such as some earthquake behavior, distribution of human travel and animal foraging patterns [1,32]. It provides a random walk whose step length obeys the Lévy distribution. Lévy distribution should be defined regarding the Fourier transform as follows:

$$F(k)=\exp\left(-\alpha|k|^{\beta}\right),\ 0<\beta\le 2 \tag{10}$$

Where α is a scale parameter. The inverse of Equation (10) is hard because it does not have an analytical form with the exception of some individual cases like β=1 or β=2.

Lévy flights are efficient in exploring unknown, large-scale space. One of the reasons is that the variance of Lévy flights is a power function, which increases very fast.

$$\sigma^2(t)\sim t^{3-\beta},\ 1\le\beta\le 2 \tag{11}$$

Figure 1 shows the path of Lévy flights for one hundred steps with β=1. It is worth noting that a power-law distribution is usually linked to some scale-free characteristics, and Lévy flights thus show self-similarity and fractal behavior in the flight patterns [31].

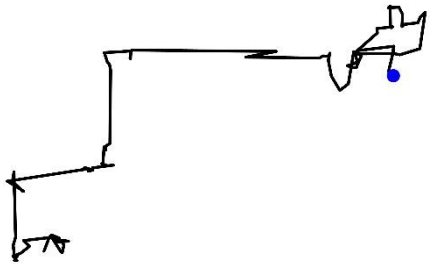

Figure 1. Lévy flights in consecutive 100 steps starting at the origin marked with ●

3.2. Cuckoo Search by Lévy Flights

Cuckoos adopt parasitic reproduction strategy to nurture their next generation. CS simulates the parasitic reproductive strategy: the solutions are seen as cuckoo eggs, the optimal solution as the cuckoo egg with the optimal fitness, the feasible region as the search zone of the cuckoos. Three idealized rules are also set as follows:

- A cuckoo only lays an egg at a time and dumps it in a nest randomly;
- The current best egg should be kept for the next generation;
- The number of the nests is fixed. The host birds should find some cuckoo eggs with a probability $P_a\in[0,1]$, and these eggs will be replaced with new eggs.

The third rule is important because it helps CS jump out of the local optimum just like the variation of GA. In this paper, finding the max LSNR is our objective. For this maximization problem, the greater the objective function value, the better the fitness.

New solutions are produced from old solutions. The update by Lévy flights is performed as [31,33]:

$$\begin{cases} x_i^{(t+1)} = x_i^{(t)} + s \\ s \sim R\dfrac{u}{|v|^{1/\beta}}\left(x_i^{(t)} - x_{best}^{(t)}\right), \quad i = 1,2,\cdots,n \\ u \sim N\left(0,\sigma_u^2\right), \sigma_u^2 = \left[\dfrac{\Gamma(1+\beta)\sin(\pi\beta/2)}{\Gamma[(1+\beta)/2]\beta 2^{(1+\beta)/2}}\right]^{1/\beta} \\ v \sim N(0,1) \quad , \sigma_v^2 = 1 \end{cases} \tag{12}$$

where $x_i^{(t+1)}$ is the *i*-th cuckoo egg of the (t+1)-th generation; $x_i^{(t)}$ is the *i*-th cuckoo egg of the *t*-th generation; *s* is the step length; *R* is the step-size scale; $x_{best}^{(t)}$ is the optimal cuckoo egg among the whole eggs of the *t*-th generation; *u* and *v* obey Gaussian distribution; $\Gamma(\cdot)$ is the standard gamma function; *n* is the number of the nests; β is a constant and equal to 1.5 in this paper.

Based on these three idealized rules and the necessary steps, CS can be summarized as the pseudo code shown in Figure 2.

Objective function $f(\boldsymbol{X})$, $\boldsymbol{X}=(x_1, \cdots, x_d)^T$;
Set the parameters including G_{max}, n, R, P_a, lower and upper border of solutions (Lb and Ub), et al.;
Generate an initial population of n host nests $\boldsymbol{X}_i$;
While (Iteration $g \le G_{max}$) or (stop criterion)
  Generate a new cuckoo nest (say i) by Lévy flights according to Equation (12), and evaluate the fitness $LSNR_i$ of new cuckoo nest according to Equations (6) and (8);
  Choose a nest among n (say j) randomly and evaluate its fitness $LSNR_j$ according to Equations (6) and (8);
  If ($LSNR_i > LSNR_j$)
    Replace nest j by the new nest;
  End
  Abandon a fraction of worse nests with a probability P_a, and build the new ones;
  Keep the best nest;
  Rank the nests and find the current best;
End while
Postprocess result and visualization

Figure 2. Pseudo code of the Cuckoo Search

3.3. Primary Technical Process of the Proposed Method

For bearing fault diagnosis, bi-stable SR with proper parameters *H* and *K* can be used to enhance the fault frequency. CS is used to find the best parameters *H* and *K*. In practice, the vibration signals of the fault bearings are too sick, and even the fault frequency cannot be found in the spectrum. Therefore, preprocessing technologies of bearing signal is needed. To express the proposed method clearly, Figure 3 shows the primary technical process of our proposed method.

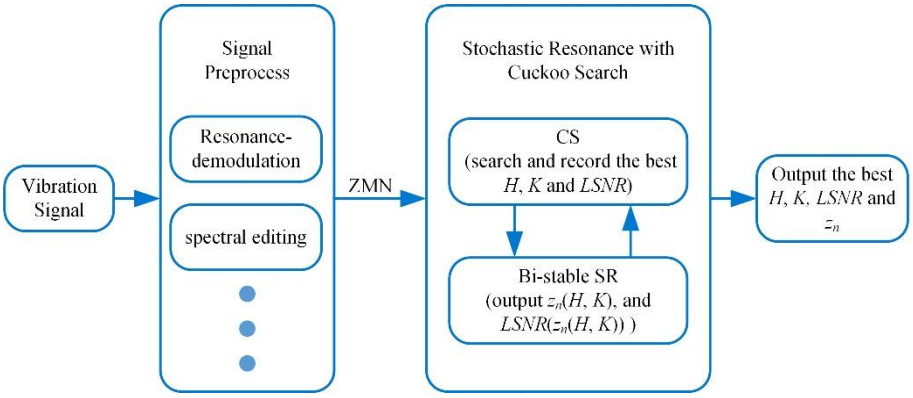

Figure 3. Primary Technical Process of the Proposed Method

The primary technical process is divided into two parts: signal preprocess and SR with CS. The first part is signal preprocess. Resonance demodulation technology is a preprocessing technology for bearing fault diagnosis. Both SK and visual

identification can help find the resonance zone. Visual identification is used to find the resonance zone in this paper. Of course, SK can be used to find a better resonance zone. The envelope signal after resonance-demodulation may contain other high-frequency components except for the fault frequency components, such as rotating frequency. These high-frequency components will influence the system output of bi-stable SR. Therefore, they should be removed by a spectrum editing method or another method. After preprocessing the vibration signal, the envelop signal should be operated by zero mean normalization (ZMN). ZMN is a typical operation, which is helpful for the realization of SR. Its expression is: x(k)-mean(x). Then, the signal after ZMN will input the second part: SR with CS. In this part, CS quickly searches the best parameters of SR such as H and K and records them. SR gives the system output z_n and $LSNR(z_n)$ according to the parameters H and K, which are provided by CS. The best H, K, $LSNR$, and z_n will be output until CS ends.

4. Experimental Analysis

To verify the feasibility of the proposed method, two bearing preset failure tests will be carried out through the mechanical failure simulation test bench as shown in Figure 4. The type of the bearing is ER-12K, and its main dimensions and characteristic failure parameters are shown in Table 1. The fault types are internal circle faults (a deep groove with 0.5 mm width in internal ring center position) and rolling faults (a deep groove with 0.5 mm width in one of the rolling element). The fault bearing is located in bearing 1.

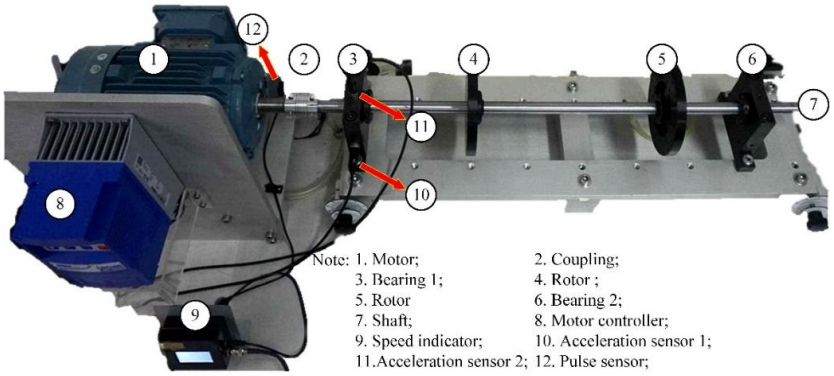

Figure 4. Part of the mechanical failure simulation test bench

Table 1. The principal dimensions and characteristic failure parameters of Bearing ER-12K

Number of R. E	R. E. Dia	Pitch Dia.	BPFI	BPFO	BSF
8	0.3125	1.318	4.950	3.048	1.992

Table 2. Parameters of each algorithm

Algorithms	Parameters
CS	P_a=0.25; Population Size=50; β=1.5
PSO	Population Size=50; Intertia Coefficient=0.99; Damping Ratio of Inertia Coefficient=0.99; Personal Acceleration Coefficient=5; Social Acceleration Coefficient=10;
GA	Population Size=100; Crossover Percentage=0.7; Extra Range Factor for Crossover=0.4; Mutation Percentage=0.3; Mutation Rate=0.1
FA	Number of Fireflies=20; Light Absorption Coefficient=1; Attraction Coefficient Base Value=2; Mutation Coefficient=0.2; Mutation Coefficient Damping Ratio=0.98; Uniform Mutation Range=0.05·(VarMax-VarMin);
ACO	Population Size=50; Sample Size=40; Intensification Factor=0.5; Deviation-Distance Ratio=1;

The data from these tests will be enhanced by bi-stable SR. The key to the objective function Equation (9) will be looked for by CS, PSO, GA, FA, and ACO. In this paper, the parameters of each algorithm are set as Table 2. Their results will be compared and analyzed. The parameters of SR are set as $H \in [10^{-2}, 10^{2}]$, $K \in [10^{-5}, 10^{4}]$.

To avoid the influence of computer performance on computing time, the same computer is used. Computer configurations are as follows: CPU is Intel Core i5-6300HQ, RAM has 16GB, and the operating system is WIN7 64. MATLAB 2017a is the calculation software. All algorithms do not use parallel computing.

4.1. Verification by Internal Ring Failure Signal

The set of the internal ring failure is produced by acceleration sensor 1. The motor speed is set at 30 rounds per second, which means the f_{BPFI}=148.50 Hz. The sampling frequency is 12800 Hz. Signal length is 4096. The resonance demodulation method

is used for preprocessing of signals. At first, the signals are filtered by minimum-order Butterworth band-pass filter. The range of the band-pass filter is [1500, 5000] Hz. The signal after filtering is the red line in Figure 5(a). The envelope signal is obtained through the Hilbert transform, as shown in Figure 5(a) (the blue line), and its spectrum is shown in Figure 5(b). The rotating frequency f_R and $2f_R$ are evident, which will influence the effect of SR. Thus, f_R and $2f_R$ will be eliminated by the spectral editing method. The signal after spectral editing and its spectrum are shown in Figure 5(c) and (d). The LSNR of the signal after spectral editing is -0.79. Comparing Figure 5(b) and (d), it is obvious that f_R and $2f_R$ disappeared, and only frequency f_{BPFI} and noise remain. The signal after spectral editing is regarded as the sum of the useful signal and the noise.

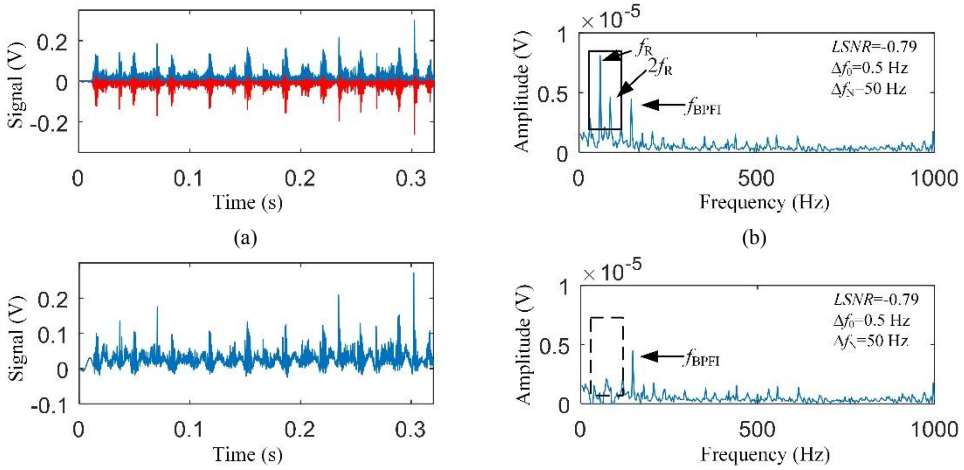

Figure 5. Signals and spectrums (a)Vibration signal after filtering (pass-band [1500,2500] Hz) and its envelope signal; (b)Spectrum of the envelope signal; (c) Signal after spectrum editing; (d) Spectrum of the signal after spectrum editing.

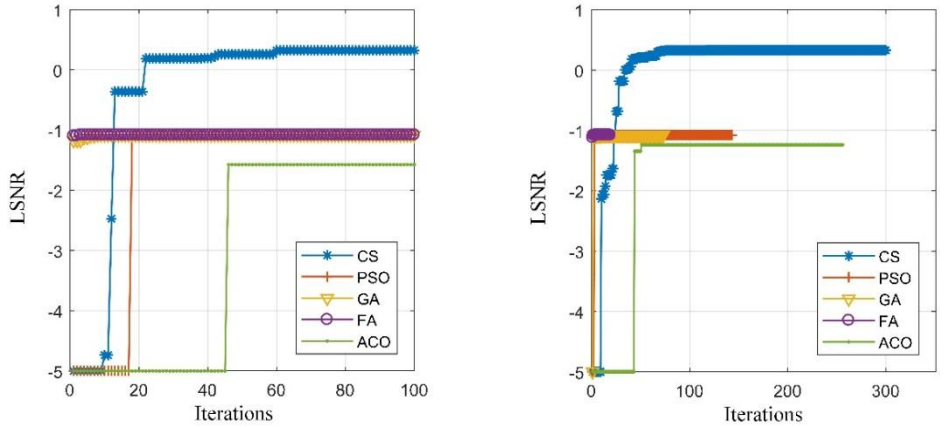

Figure 6. The fitness convergence curves of the whole algorithms (internal ring failure signal) (a) Max iterations=100 time; (b) Computation Time=120s

The envelope signal is input to the bi-stable system after ZMN, and the max *LSNR* is searched by CS, PSO, GA, FA, and ACO respectively. Considering the influence of the max iteration times and the computation time of every algorithm, two situations are analyzed. One is that the max iteration period of all algorithms is the same and equal to 100 times. The other one is that the computation time of every algorithm is limited to 120s. When the LSNR is smaller than -5, we let LSNR be -5. The fitness convergence curves of the whole algorithms in the two situations are shown in Figure 6(a) and (b). The optimization results are presented in Table 3. From Figure 6(a) and (b), we can find that the convergence curve of CS is steep in the early stage of optimization, which indicates that the CS converges quickly. Furthermore, the convergence curve of CS is the highest among all the cures in the end stage of optimization, which shows that CS has the best performance for searching the optimal global solution. From Table 3, we can find that when the max iteration is the same, the computation time of CS is equal to 31.87 s, which is the shortest of all the algorithms. When the computation time is the same, the number the iteration is equal to 300 times, which is the most. Thus, CS is a simple algorithm and can calculate very quickly. Furthermore, the LSNR of the signal optimized by CS is the biggest and equal to 0.32. Thus, the quality of the output signal through SR-based CS is the best. However, LSNRs based on other algorithms are less than the LSNR of the envelope signal (-0.79), which indicates that SR is not triggered. Figure 7(a) and (b) show the output signal ant its spectrum (when [*H, K*]=[0.11, 47.27]). Comparing the Figure

7(b) with Figure 5(d), the frequency f_{BPFI} is more obvious. The LSNR of the signal is enhanced from -0.79 to 0.32. Thus, the SR is very effective. The spectrum of the signal as shown in the black box of Figure 7(b) becomes abundant, which is caused by Lorentz effect.

Table 3. Optimization results of the five algorithms and related parameters

Algorithms	Limitation: Max Iterations=100 times			Limitation: Computation Time=120s		
	Used time/s	LSNR	[*H, K*]	Iterations	LSNR	[*H, K*]
CS	31.87	0.32	[0.11, 47.27]	300	0.32	[0.11, 46.80]
PSO	77.00	-1.08	[0.01, 5190.62]	143	-1.08	[0.01, 5190.97]
GA	168.29	-1.08	[0.01, 5189.18]	73	-1.08	[0.01, 5189.22]
FA	274.06	-1.08	[0.01, 5189.18]	19	-1.08	[0.01, 5189.18]
ACO	46.21	-1.57	[0.064, 293.87]	256	-1.24	[82.54, 4469.85]

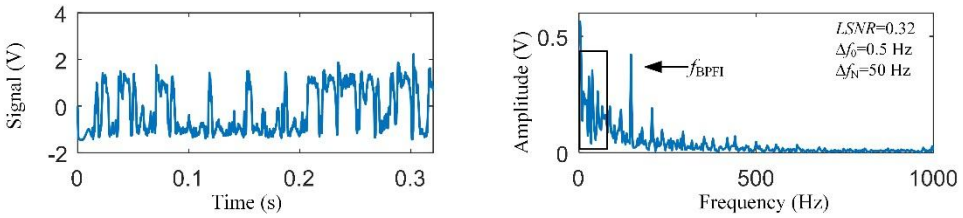

(a) (b)

Figure 7. (a) The output signal after SR ([*H, K*] = [0.11, 47.27]) and (b) its spectrum through the proposed method

4.2. Verification by Rolling Element Failure Signal

The characteristic failure frequency of bearing internal ring fault signal is evident and enhanced fatherly through SR. However, sometimes the characteristic failure frequency is weak and submerged in the intense noise background. The rolling element failure signal is just this situation. The motor speed is set at 30 rounds per second, which means the f_{BSF}=59.76 Hz. The sampling frequency is 12800 Hz. Signal length is 3200. The signal after band-pass filtering ([1000, 2500] Hz) is the red line as shown in Figure 9(a). The blue line in Figure 9(a) is the envelope signal, and its spectrum is shown in Figure 9(b). The LSNR of the envelope signal is only -12.13. The characteristic failure frequency f_{BSF} is submerged in the noise. The envelope signal is input to the bi-stable system after ZMN, and CS, PSO, GA, FA, and ACO are also used to find the solution of Equation (9). The parameters of every algorithm are also shown in Table 2, and feasible region of Equation (9) is also that of $H \in [10^{-2}, 10^{2}]$ and $K \in [10^{-5}, 10^{4}]$. The max iterations and the computation time are also under consideration. The fitness convergence curves in the two situations are as shown in Figure 8 (When the LSNR is smaller than -20, we let LSNR be -20). The curves of CS are steep in the early stage and highest in the end stage in Figure 8. Therefore, the fitness of the CS converges quickly, and the optimization result is the best among the algorithms in this case. When the computation time is about 120 s, the convergence curve of CS is the longest. That is to say that the iterations of CS are the most, which means that CS is very simple. After optimization by CS with 120 seconds, the LSNR of the output signal becomes -0.83 and the optimal parameters [*H, K*]=[1.94, 9119.68]. The output signal and its spectrum are shown in Figure 9(c) and (d). Comparing Figure 9(b) and (d), the characteristic failure frequency f_{BSF} is strengthened. Thus, SR can enhance the weak signal submerged in the strong noise background.

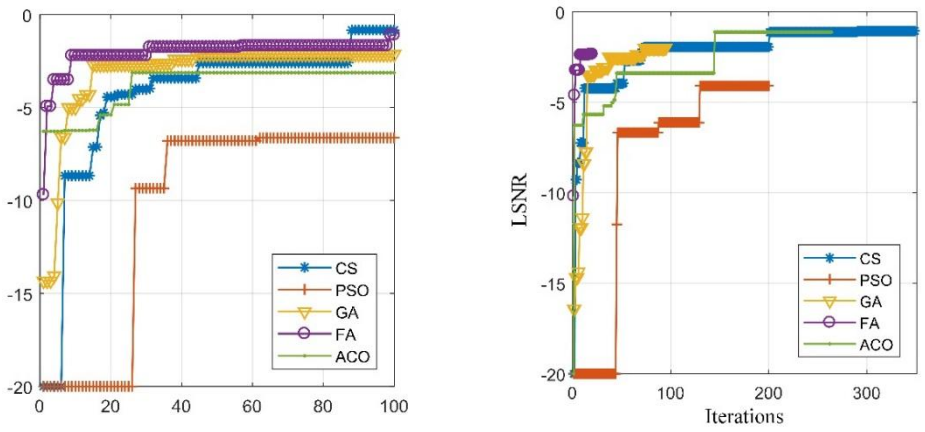

(a) (b)

Figure 8. The fitness convergence curves of the whole algorithms (rolling element failure signal) (a) Max iterations=100 time; (b) Computation Time=120s

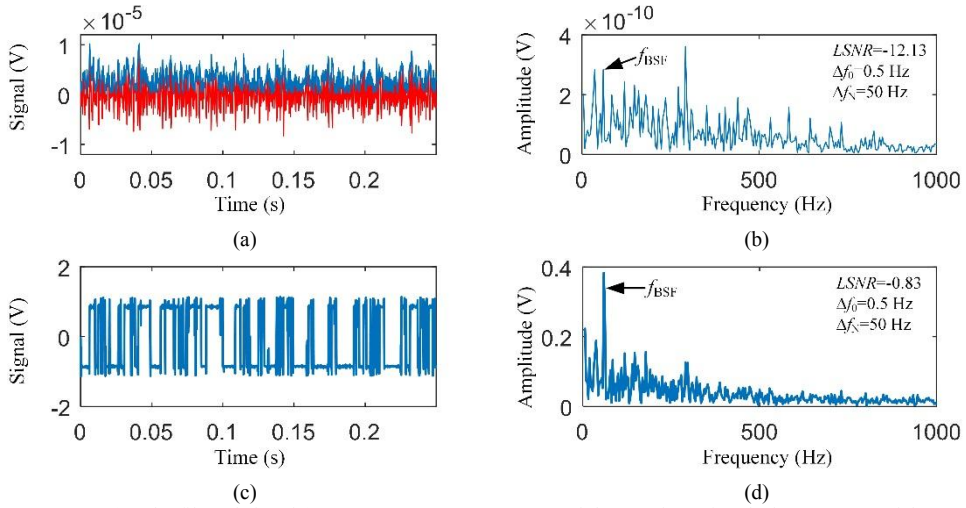

Figure 9. Signals ant spectrums (a) The filtered signal (pass-band [1000, 2500] Hz) and the envelope signal; (b) Spectrum of the envelope signal; (c) The output signal after SR ([*H*, *K*]=[1.94, 9119.68]); (d) Spectrum of the output signal

5. Conclusions

Due to the characteristic of using noise to amplify useful signal rather than eliminating noise, SR has aroused great concern in the field of mechanical fault diagnosis. The effect of SR is affected not only by noise intensity, but also by nonlinear system parameters. Because of the advantages of CS, such as short computation time, fast convergence and excellent global searchability, this paper proposed a novel parameter-induced SR based on CS and applied it to fault detection for rolling bearings. LSNR is regarded as the evaluating indicator of SR. The fault data of the bearing internal ring and the data of the rolling element are collected. SR methods based on CS, GA, PSO, FA, and ACO are used to analyze the two datasets. The results show that the SR method based on CS can find the better LSNR regardless of if it is in the same iterations or in the same computation time, and the output signal is improved.

Acknowledgements

This research was supported in part by the Natural Science Foundation of Hebei Province (No. E2015506012).

References

1. P. Barthelemy, J. Bertolotti, and D. S. Wiersma, “A Levy flight for light,” *Nature*, vol. 453, no. 7194, pp. 495-498, 2008
2. R. Bates, O. Blyuss, and A. Zaikin, "Stochastic resonance in an intracellular genetic perceptron," *Physical Review E,* (online since March 26 2014) (DOI 10.1103/PhysRevE.89.032716)
3. R. Benzit, A. Sutera, and A. Vulpiani, “The mechanism of stochastic resonance,” *Journal of Physics A: Mathematical and General*, vol. 8, no. 7, pp. 62-67, 1981
4. K. Chi, J. Kang, K. Wu, and X. Wang, “Bayesian Parameter Estimation of Weibull Mixtures Using Cuckoo Search,” in *8-th International Conference on Intelligent Networking and Collaborative Systems*, pp. 411-414, Ostrava, Czech Republic, September 2016
5. M. Dorigo, M. Birattari, and T. Stutzle, “Ant colony optimization,” *IEEE Computational Intelligence Magazine*, vol. 1, no. 4, pp. 28-39, 2006
6. F. Duan, and B. Xu, “PARAMETER-INDUCED STOCHASTIC RESONANCE AND BASEBAND BINARY PAM SIGNALS TRANSMISSION OVER AN AWGN CHANNEL,” *International Journal of Bifurcation and Chaos*, vol. 13, no. 2, pp. 411-425, 2003
7. L. Gammaitoni, P. Hänggi, P. Jung, and F. Marchesoni, “Stochastic resonance,” *Review of Modern Physics*, vol. 70, no. 1, pp. 223-287, 1998
8. D. E. Goldberg, and J. H. Holland, “Genetic Algorithms and Machine Learning,” *Machine Learning*, vol. 3, no. 2-3, pp. 95-99, 1988
9. D. He, X. Wang, S. Li, J. Lin, and M. Zhao, “Identification of multiple faults in rotating machinery based on minimum entropy deconvolution combined with spectral kurtosis,” *Mechanical Systems and Signal Processing*, vol. 81, pp. 235-249, 2016
10. Q. He, J. Wang, Y. Liu, D. Dai, and F. Kong, “Multiscale noise tuning of stochastic resonance for enhanced fault diagnosis in rotating machines,” *Mechanical Systems & Signal Processing*, vol. 28, no. 2, pp. 443-457, 2012
11. N. Hu, M. Chen, G. Qin, L. Xia, Z. Pan, and Z. Feng, “Extended stochastic resonance (SR) and its applications in weak mechanical signal processing,” *Frontiers of Mechanical Engineering in China*, vol. 4, no. 4, pp. 450-461, 2009

12. Y. Lei, D. Han, J. Lin, and Z. He, "Planetary gearbox fault diagnosis using an adaptive stochastic resonance method," *Mechanical Systems & Signal Processing*, vol. 38, no. 1, pp. 113-124, 2013
13. Y. Lei, Z. Qiao, X. Xu, J. Lin, and S. Niu, "An underdamped stochastic resonance method with stable-state matching for incipient fault diagnosis of rolling element bearings," *Mechanical Systems & Signal Processing*, vol. 94, pp. 148-164, 2017
14. Y. G. Leng, Y. S. Leng, T. Y. Wang, and Y. Guo, "Numerical analysis and engineering application of large parameter stochastic resonance," *Journal of Sound & Vibration*, vol. 292, no. 3-5, pp. 788-801, 2006
15. J. Li, X. Chen, and Z. He, "Adaptive stochastic resonance method for impact signal detection based on sliding window," *Mechanical Systems & Signal Processing*, vol. 36, no. 2, pp. 240-255, 2013
16. M. Lin, and Y. M. Huang, "Modulation and demodulation for detecting weak periodic signal of stochastic resonance," *Acta Physica Sinica*, vol. 55, no. 7, pp. 3277-3283, 2006
17. J. J. Liu, Y. G. Leng, Z. H. Lai, and D. Tan, "Stochastic resonance based on frequency information exchange," *Acta Physica Sinica*, (online since November 20 2016) (DOI 10.7498/aps.65.220501)
18. S. Lu, Q. He, H. Zhang, and F. Kong, "Rotating machine fault diagnosis through enhanced stochastic resonance by full-wave signal construction," *Mechanical Systems & Signal Processing*, no. 85, pp. 82-97, 2016
19. S. Łukasik, and S. Żak, "Firefly Algorithm for Continuous Constrained Optimization Tasks," in *International Conference on Computational Collective Intelligence*, pp. 97-106, Wroclaw, Poland, October 2009
20. M. Malik, F. Ahsan, and S. Mohsin, "Adaptive image denoising using cuckoo algorithm," *soft computing*, vol. 20, no. 3, pp. 925-938, 2016
21. B. Mcnamara, and K. Wiesenfeld, "Theory of stochastic resonance," *Physical Review A*, vol. 39, no. 9, pp. 4854-4869, 1989
22. M. K. Naik, and R. Panda, "A novel adaptive cuckoo search algorithm for intrinsic discriminant analysis based face recognition," *Applied Soft Computing*, vol. 38, pp. 661-675, 2016
23. A. Ouaarab, B. Ahiod, and X. Yang, "Discrete cuckoo search algorithm for the travelling salesman problem," *Neural Computing and Applications*, vol. 24, pp. 1659-1669, 2014
24. R. Poli, J. Kennedy, and T. Blackwell, "Particle swarm optimization An overview," *Swarm Intelligence*, vol. 1, no. 1, pp. 33-57, 2007
25. A. S. Raj, and N. Murali, "Morlet Wavelet UDWT Denoising and EMD based Bearing Fault Diagnosis," *Electronics*, vol. 17, no. 1, pp. 1-8, 2013
26. R. B. Randall, and J. Antoni, "Rolling element bearing diagnostics—A tutorial," *Mechanical Systems and Signal Processing*, vol. 25, no. 2, pp. 485-520, 2011
27. N. Sawalhi, R. B. Randall, and H. Endo, "The enhancement of fault detection and diagnosis in rolling element bearings using minimum entropy deconvolution combined with spectral kurtosis," *Mechanical Systems & Signal Processing*, vol. 21, no. 6, pp. 2616-2633, 2007
28. P. Shi, X. Ding, and D. Han, "Study on multi-frequency weak signal detection method based on stochastic resonance tuning by multi-scale noise," *Measurement*, vol. 47, pp. 540-546, 2014
29. J. Tan, X. Chen, J. Wang, H. Chen, H. Cao, Y. Zi, and Z. He, "Study of frequency-shifted and re-scaling stochastic resonance and its application to fault diagnosis," *Mechanical Systems and Signal Processing*, vol. 23, no. 3, pp. 811-822, 2009
30. J. Wang, Q. He, and F. Kong, "Adaptive Multiscale Noise Tuning Stochastic Resonance for Health Diagnosis of Rolling Element Bearings," *IEEE Transactions on Instrumentation & Measurement*, vol. 64, no. 2, pp. 564-577, 2015
31. X. Yang, "Nature-Inspired Metaheuristic Algorithms Second Edition," Luniver Press, London, 2010
32. X. Yang, and S. Deb, "Cuckoo Search via Lévy flights," in *World Congress on Nature and Biologically Inspired Computing*, pp. 210-214, Coimbatore, India, December 2009
33. X. Yang, and S. Deb, "Multiobjective cuckoo search for design optimization," *Computers & Operations Research*, vol. 40, no. 6, pp. 1616-1624, 2013
34. Y. Yang, Z. P. Jiang, B. Xu, and D. W. Repperger, "An investigation of two-dimensional parameter-induced stochastic resonance and applications in nonlinear image processing," *Journal of Physics A*, vol. 42, no. 14, pp. 145207, 2009
35. X. Zhang, N. Q. Hu, Z. Cheng, and L. Hu, "Enhanced Detection of Rolling Element Bearing Fault Based on Stochastic Resonance," *Chinese Journal of Mechanical Engineering*, vol. 25, no. 6, pp. 1287-1297, 2012
36. X. Zhang, J. Kang, J. Zhao, and H. Teng, "Rolling element bearings fault diagnosis based on correlated kurtosis kurtogram," *Journal of Vibroengineering*, vol. 17, no. 6, pp. 3023-3034, 2015
37. X. Zhang, J. Kang, L. Xiao, J. Zhao, and H. Teng, "A New Improved Kurtogram and Its Application to Bearing Fault Diagnosis," *Shock & Vibration*, vol. 2015, pp. 1-22, 2015
38. X. H. Zhang, J. S. Kang, L. S. Hao, L. Y. Cai, and J. M. Zhao, "Bearing fault diagnosis and degradation analysis based on improved empirical mode decomposition and maximum correlated kurtosis deconvolution," *Journal of Vibroengineering*, vol. 17, no. 1, pp. 243-260, 2015
39. Z. H. Zhang, D. Wang, T. Y. Wang, J. Z. Lin, and Y. X. Jiang, "Self-adaptive step-changed stochastic resonance using particle swarm optimization," *Journal of Vibration & Shock*, vol. 32, no. 19, pp. 125-130, 2013

Kuo Chi received the B.Sc. degree in Mechanical engineering from Jimei University, Xiamen, China, in 2013 and M.S. degree in Maintenance Engineering from Mechanical Engineering College, Shijiazhuang, China, in 2015. He is a Ph.D. student of Mechanical Engineering College, Shijiazhuang, China. His research is focused on fault detection, diagnostics and prognostics, and performance-based contracting.

Jianshe Yang received his Ph.D. degree in Mechatronical Engineering from Beijing Institute Technology, Beijing, China. He is a professor at Mechanical Engineering College, Shijiazhuang, China. His research interests include reliability analysis and optimization, and condition monitoring.

Xinghui Zhang received his B.Sc. degree, M.S. degree and Ph.D. degree in Management Engineering from Mechanical Engineering College, Shijiazhuang, China, in 2005, 2010 and 2015. He currently works as a Postdoctor at Mechanical Engineering College, Shijiazhuang, China. His research is focused on fault detection, diagnostics and prognostics, and performance-based contracting.

Zhiyuan Yang received his B.Sc. degree in Management engineering from Nankai University, Tianjin, China, in 2013 and M.S. degree in Maintenance Engineering from Mechanical Engineering College, Shijiazhuang, China, in 2015. He is a Ph.D. student at Mechanical Engineering College, Shijiazhuang, China. His research is focused on maintenance decision and equipment health management.